**Eur**opean **J**ournal of **Chem**istry

# A corrected benzene nitration three-step mechanism derived by DFT calculation and MO theory

Hongchang Shi 🆔 *

*Department of Chemistry, Tsinghua University, Beijing 100084, China*

* Corresponding author at: Department of Chemistry, Tsinghua University, Beijing 100084, China.
 e-mail: shihc@mail.tsinghua.edu.cn (H. Shi).

**RESEARCH ARTICLE**

**ABSTRACT**

Density-functional theory (DFT) calculations at the LC-wHPBE/6-311++G(d,p) level found that the textbook three-step nitration mechanism of benzene in mixed acids was seriously wrong. Step 1 of generating nitronium ion ($NO_2^+$) is not spontaneous, the $NO_2^+$ is generated by Lewis collision, and needs to overcome a barrier $E_a$ = 18 or 22 kcal/mol in mixed acid or in nitric acid. Obtaining the $E_a$ of the Lewis collision by quantum chemical calculations is a highlight of the study. The reaction system ($NO_2^+ + H_2O$) + $HSO_4^-$ or + $NO_3^-$ or + $nH_2O$ ($n \geq 1$) can make $NO_2^+$ spontaneously change to $HNO_3$ through a poly($\geq 3$)-molecular acidification. Sulfuric acid can greatly reduce [$H_2O$] and increase [$NO_2^+$]. Therefore, the nitration rate in mixed acid is much faster than that in nitric acid. Step 2, $C_6H_6 + NO_2^+$, is an electrophilic addition, follows the transition state theory, and needs to overcome a low barrier, $\Delta E^*$ = 7 kcal/mol. The product of Step 2 is the σ-complex $C_6H_6$-$NO_2^+$. The essence of the electrophilic addition is the transfer of HOMO-1 electrons of $C_6H_6$ to LUMO of $NO_2^+$. Step 3 is a spontaneous Lewis acid-base neutralization without any barrier, and generates the target product nitrobenzene $C_6H_5NO_2$. $NO_2^+$ and σ-complex are the two active intermediates in nitration. The benzene nitration rate control step is not Step 2 of generating σ-complex, but is Step 1 to generate $NO_2^+$. The DFT calculation obtains the barriers $E_a$ and $\Delta E^*$, the reaction heats $\Delta H_\sigma$ and $\Delta H_p$ of each step of the nitration, resulting in the total nitration reaction heat $\Delta H$ = -35 kcal/mol. It is consistent with the experimental $\Delta H$ = -34 kcal/mol. Based on the results, a corrected benzene nitration three-step mechanism proposed.

**Journal website**: www.eurjchem.com

## 1. Introduction

The nitration of benzene in mixed acid is an important reaction in the electrophilic substitution of aromatics, and thus it is always an indispensable content in the authoritative general or advanced organic chemistry textbooks [1-6]. Benzene reacts slowly with hot concentrated nitric acid to yield nitrobenzene, but if the reaction is carried out by benzene with a hot mixture (usually 1:2-4) of concentrated nitric acid and sulfuric acid, then it is much faster as the following Equation (1). In nitration, sulfuric acid is not consumed, but it greatly accelerates the reaction.

Over a hundred years, the nitration reaction mechanism has been extensively investigated. In 1904, Euler [7] suggested that the nitronium ion ($NO_2^+$) is the nitrating agent. The classic aromatic nitration mechanism finally was established through subsequent large number of studies from many chemists [8-20], which took about half a century. Among them, the contribution of the Ingold group [12-20] to the mechanism is the largest. In organic chemistry textbooks [1-6], the classic nitration mechanism is shown as Scheme 1.

Step **1** (Scheme 1) is the hydroxyl oxygen of $HNO_3$ being protonated by $H_2SO_4$ in the mixed acid to generate $NO_2^+$, and is a chemical equilibrium without any barrier. However, Step **1** means that $HNO_3$ reacts with two $H_2SO_4$ molecules, and it is able

to generate another positive ion $H_3O^+$ and another negative ion $HSO_4^-$. However, there is a key question without answer: is the left → right spontaneous or need to overcome a barrier for the generation of $NO_2^+$? If there is a barrier, is it how high? As early as 1945, Ingold [21] had raised the question; Forming $NO_2^+$ may be '*unimolecular*' or '*bimolecular*', according as the heterolysis of the nitric acid molecule to yield the $NO_2^+$ is rate-determining step or not? But in 1950, Ingold, based on the $N_2O_5$-$H_2O$ freezing point diagram, concluded that the $NO_2^+$ ion is generated by an automatic proton transfer and an ion self-dissociation of the 2 $HNO_3$ (Equation (2)) [13,16].

In March's advanced organic textbook [5], the $HNO_3$ + $2H_2SO_4$ and $HNO_3$ + $HNO_3$ are even considered as an acid-base reaction. Apparently, he also thinks that the formation of $NO_2^+$ is achieved by automatic or spontaneous proton transfer to form $O_2N$-$OH_2^+$, then dissociated into $NO_2^+$. Therefore, the generation of $NO_2^+$ in Step **1** (Scheme 1) has always considered as a spontaneous process without barrier. But the nitration is carried out at 50-60 °C, there must be a barrier, and thus the barrier is judged to appear in Steps **2** and **3** in Scheme 1. In organic chemistry textbooks, Step **2** marks by the adjective, *slow*, showing that Step **2** is the rate-controlling step. In Step **3**, the σ-complex transfers the H proton of benzene ring to $HSO_4^-$ or $H_2O$, it is considered as also need to overcome a barrier, but its barrier is lower than that of Step **2**, thus mark by the
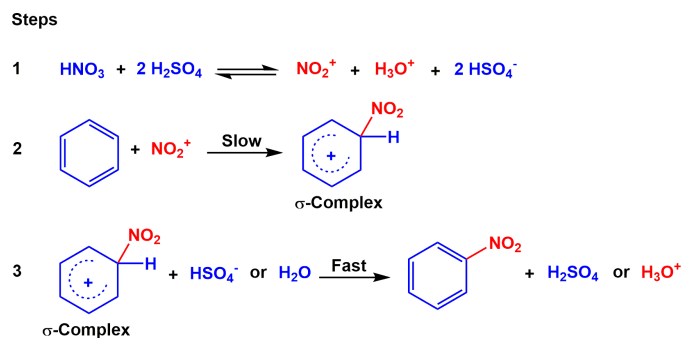
**Scheme 1.** The popular textbook three-step nitration mechanism of benzene in mixed acid.



$$2\ HNO_3 \rightarrow O_2N\text{-}OH_2^+ + NO_3^- \rightarrow O_2N^+ + H_2O + NO_3^- \tag{2}$$
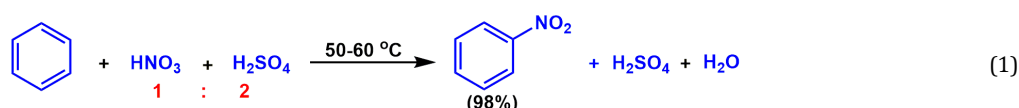
adjective, *fast*. Many textbooks often give a potential energy curve with two barriers, and the barrier of Step **2** is higher than that of Step **3**, which again shows that Step **2** is the rate-controlling step (Scheme 1).

However, $NO_2^+$ is a high-potential cation. Isn't there any barrier to be overcome for forming such an ion? In 1978, Sheats and Strachan [22] performed a kinetic study on the nitration mechanism of toluene in mixed acids. By using a stopped-flow spectrometer, they obtained the kinetic parameters of toluene nitration in 77.3 or 78.45 wt % sulfuric acid (Nitric acid: sulfuric acid ≈ 1:3.4 or 1:3.6) and the activation energy of forming $NO_2^+$ was obtained by kinetic calculation, $E_a$ = 18.3±4.0 kcal/mol. The $E_a$ of the reverse reaction is 10.5 or 12.0±4.0 kcal/mol. The $E_a$ of $CH_3$-$C_6H_5$ + $NO_2^+$ generating σ-complex is 5.9±0.1 and 6.3±0.5 kcal/mol, respectively. The results indicate that the rate control step of the nitration in mixed acids is not Step **2** in Scheme 1, but is Step **1** of generating $NO_2^+$. The barrier data of toluene nitration in mixed acid is the only experimental one in the literature so far. However, their method cannot determine which one of the two steps of forming $NO_2^+$ and σ-complex follows the transition state theory and which one follows the Lewis collision theory.

Last over 30 years, many groups have made quantum chemistry study on the aromatic nitration mechanism [23-33], but no one paid attention to how the nitronium ion $NO_2^+$ be formed, and all focus on the "*rate-controlling step*", Step **2** in Scheme 1. These *ab-initio* or DFT calculation studies on the $C_6H_6$ + $NO_2^+$ mechanism have yielded great results. The results confirmed that the $C_6H_6$ + $NO_2^+$ reaction follows the transition state theory and the product is an σ-complex (arylium ion). A recent research of Brinck group [33] is representative. They get by DFT calculation at M06-2x/6-311G(d,p) level that the addition barrier of forming the σ-complex of benzene is low, 3.1 kcal/mol ($H_2O$ as solvent), and the reaction heat is -13.0 kcal/mole.

The nitration mechanism given in Scheme 1 is a three-step process, $NO_2^+$ and the σ-complex are two active intermediates, and these contents are correct. However, the DFT calculations show that the rate-controlling step of the benzene nitration is not Step **2** of generating σ-complex, but is Step **1** of generating $NO_2^+$. Step **3** of generating the target product is a spontaneous Lewis acid-base neutralization without any barrier.

## 2. Computational methods and frontier orbital theory

The DFT computation was carried out with Gaussian 16, Revision B.01 program [34] and DFT methods. LC-wHPBE [35] is a recommended version of the long-range corrected ωPBE functional. In 2014, Galano [36] found that LC-wHPBE was the best among 18 functional for kinetic calculations of radical reactions by using 6-311++G(d,p) basis set and experimental data as reference; and found that the second best functional is M06-2x [37]. One of our recent research on the solvolysis mechanism [38] of *t*-butyl chloride or bromide shows that the LC-wHPBE also is a suitable functional. Considering that benzene is a large conjugate molecule, the hydroxyl group of $H_2O$ is a key active group, and negative ions ($HSO_4^-$, $NO_3^-$) appear in the nitration, the DFT calculation also uses the 6-311++G(d,p) basis set.

Kenichi Fukui's frontier orbital theory (FO) [39-41] is the most widely used molecular orbital theory (MO) to demonstrate the electron transfer process of many organic reactions. In the frontier orbital theory (FO), the bonding three-principles [42] are the basic conditions for chemical bonding, of which symmetry matching is the most critical. In order to show the electron transfer process in nitration, many structures are attached with their HOMO and LUMO images. However, for organic reactions, especially poly-molecular reactions, the frontier MOs are diverse. The HOMO-1 or LUMO+1 or other MOs are also often frontier MOs.

The solvent of the nitration reaction is a mixture of containing strong polar $HNO_3$, $H_2SO_4$, $H_2O$ and product $C_6H_5NO_2$. Nitration is carried out in such a solvent, and thus the solvent effect must be included in the DFT calculation. However, the Gaussian program cannot calculate the solvent effect of the two strong acids. In order to estimate the solvent effect of the nitration, $HCONH_2$ (ε = 108.9) is used as solvents to perform the simulation calculation. $HCONH_2$ was chosen because it has the highest polarity ($H_2SO_4$ ε ≅ 100), and it had already been used in a study [32] of the benzene nitration mechanism performed by DFT calculation. The Tomasi's polarizable continuum model IEFPCM [43-46] is used to calculate the solvent effects.

In the study, the energies obtained by the DFT calculation all have included the zero-point correction and the thermal correction to the Gibbs free energy, which allows the calculation to obtain the $E_a$ and $\Delta E^*$, reaction heat $\Delta H_\sigma$ and $\Delta H_p$ of the three

**Steps**

1    $HNO_3 + H_2SO_4 \rightleftharpoons H_2O^+\text{-}NO_2 + HSO_4^-$

2    $H_2O^+\text{-}NO_2 \rightleftharpoons NO_2^+ + H_2O$

3    $H_2O + H_2SO_4 \rightleftharpoons H_3O^+ + HSO_4^-$

$$HNO_3 + 2\,H_2SO_4 \rightleftharpoons NO_2^+ + H_3O^+ + 2\,HSO_4^-$$
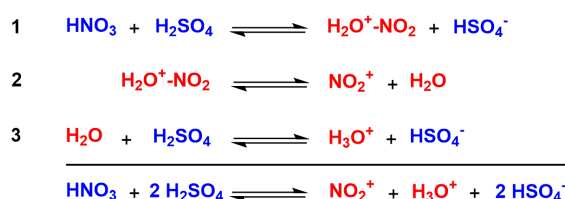
**Scheme 2.** Generating $NO_2^+$ and $H_3O^+$ by $HNO_3 + 2H_2SO_4$ in the textbook mechanism.

(a) $H_2SO_4 \rightleftharpoons HSO_4^- + H^+$

(b) $HO\text{-}NO_2 + H^+ \rightleftharpoons H_2O^+\text{-}NO_2$             (3)

$$H_2SO_4 + n\,H_2O \xrightarrow[\text{Spontaneous}]{n \geq 3} (n\text{-}1)\,H_2O \cdots H_3O^+ + HSO_4^- \qquad (4)$$
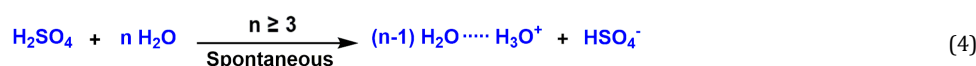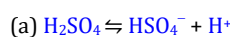
steps at default 298.15 K, and enables the data obtained from the DFT calculation to be compared with the experimental data.

## 3. Results and discussions

### 3.1. Generation of $NO_2^+$ in textbook mechanism is a wrong description

For the nitration of benzene, the electrophile $NO_2^+$ must first be generated, as shown in Step **1** in Scheme 1. Step **1** is a reaction between one nitric acid and two sulfuric acid molecules. The product is 1 $NO_2^+$, 1 $H_3O^+$, and 2 $HSO_4^-$. How did the $NO_2^+$ and $H_3O^+$ formed? Some textbooks [1,4] already explain: Step **1** in Scheme 1 is a three-step reaction as shown in Scheme 2. Step **1** in Scheme 2 generates a key active intermediate through the automatic proton transfer to $HNO_3$, σ-complex $H_2O^+\text{-}NO_2$. Step **2** in Scheme 2 is the formation of $NO_2^+$ by a spontaneous dissociation of the σ-complex. Finally, another product $H_2O$ from Step **2** in Scheme 2 is protonated by the second $H_2SO_4$ molecule to form $H_3O^+$ in Step **3** (Scheme 2).

However, the study shows that the three Steps **1**-**3** in Scheme 2 all are wrong. First, the σ-complex $H_2O^+\text{-}NO_2$ cannot be formed in mixed acid. Second, here $H_2O$ cannot also be protonated by $H_2SO_4$ to $H_3O^+$ because the $H_2SO_4$ molecule is not in water but is in mixed acid. Note that, in some textbooks [1,3], Step **1** in Scheme 1 is $HNO_3 + H_2SO_4 \rightleftharpoons NO_2^+ + H_2O + HSO_4^-$, so only Steps **1** and **2** in Scheme 2 exist. Of course, these two steps are also wrong.

The DFT calculation shows that $HNO_3$ and $H_2SO_4$ or $2HNO_3$ cannot react spontaneously to form σ-complex $H_2O^+\text{-}NO_2$. Then, how is the $H_2O^+\text{-}NO_2$ in the textbooks formed? Apparently, it is a classic acid-base neutralization process [5], $HNO_3 + H_2SO_4$ is through the reaction in Equation (3).

However, in mixed acid, there is no such $H_2SO_4$ automatic dissociation to form the free $H^+$, because the O-H bond in the $H_2SO_4$ or $HNO_3$ molecule is an σ-bond with high strength, so there is no automatic protonation either.

The **1** is the optimized initial structural of $H_2SO_4$ (Figure 1) and **2** is the optimized product structure after $H_2SO_4$ being dissociated (Figure 1). From **1** and **2** (Figure 1), the dissociation energy is $\Delta E = E_1{}^* - E_1 = 0.235030$ a.u. $= 147.4$ kcal/mol. Also using *ab-initio* MP2 to perform this calculation, the $\Delta E = 0.237408$ a.u. $= 148.9$ kcal/mol. It has a high dissociation energy, indicating that it is impossible to generate free $H^+$ ion by automatic dissociation of $H_2SO_4$ in mixed acid. The dissociation of $H_2SO_4$ in Equation (3a) does not exist in mixed acid.

The **3** is an initial structural setting of σ-complex $H_2O^+\text{-}NO_2$ after $HNO_3$ is protonated by $H^+$ (Figure 1) and **4** is the optimized

structure of **3** (Figure 1). The **4** shows that the σ-bond of $H_2O^+\text{-}NO_2$ has been broken, that is, the $H_2O^+\text{-}NO_2$ become to $H_2O$ and $NO_2^+$ after optimization. A stable σ-complex will definitely exist in its optimized structure (Ex. $C_6H_6\text{-}NO_2^+$ behind). The above results show that there is no free $H^+$, also no σ-complex $H_2O^+\text{-}NO_2$ in the mixed acid. The formation of $NO_2^+$ does not occur through the dissociation of $H_2O^+\text{-}NO_2$, but rather through another pathway.

If the hydroxyl oxygen protonation of $HNO_3$ can form the $H_2O^+\text{-}NO_2$, then $H_2O + NO_2^+$ can also form the σ-complex, but why cannot the two form the σ-complex? The **5** and **6** is an optimized structure of $NO_2^+ + H_2O$ with HOMO and LUMO images and energy $E'$ (Figure 1). This is an Opt = Modredundant calculation with freezing coordinates ($H_2O \cdots NO_2^+ = 2.000$ Å).

The nature of generating σ-complex by $NO_2^+$ and $H_2O$ is the transfer of HOMO electrons of $H_2O$ to LUMO of $NO_2^+$. According to the "+*" and "-*" in the HOMO of **5** and the "-*" in the LUMO of **6**, the symmetry of the two frontier MOs non-match (Figure 1). At the same time, the energy of internuclear repulsion increases N···O approaches each other. The energy $E'$ of the systems **5** or **6** is 6.6 kcal/mole higher than the $E_1$ of **4**. If the σ-complex is set to $H_2O \cdots NO_2^+ = 1.5$ Å, the DFT calculation gives that its energy rises by 24.7 kcal/mol. These show that electron transfer HOMO → LUMO cannot occur, and therefore, even though $H_2SO_4$ can automatically form $H^+$ (Equation 3a), protonation ($HNO_3 + H^+$) cannot also form the σ-complex $H_2O\text{-}NO_2^+$. Therefore, in the generation of $NO_2^+$, the σ-complex intermediate $H_2O^+\text{-}NO_2$ does not exist in the mixed acid, that is, the two chemical equilibriums **1** and **2** in Scheme 2 are wrong.

The following needs to continue to examine the Step **3** in Scheme 2. If the $H_2SO_4$ molecule is in water, the proton of its -OH group can easily be transferred to a $H_2O$ molecule. However, the DFT calculation shows that the generation of $H_3O^+$ in water also is not a simple bimolecular reaction of $H_2SO_4 + H_2O$. It is a poly-($n \geq 4$) molecular proton-transfer process.

In Figure 2, the system **1** is the optimized initial structure of one $H_2SO_4$ molecule and three $H_2O$ molecules, and system **2** is the optimized product structure. It can be seen from **2** (Figure 2), $H_3O^+$ spontaneously formed and released reaction heat $\Delta H = E_p - E_1 = -0.018454$ a.u. $= -11.6$ kcal/mol. If the number of water molecules is increased, the bond length of the $H_3O^+$ will be shorter and the reaction heat released will increase. Therefore, $H_2SO_4$ tends to form $H_3O^+$ in water. The protonation of $H_2O$ is a spontaneous poly-molecular ($H_2SO_4 + nH_2O$, $n \geq 3$) proton transfer. The generation of $H_3O^+$ can be expressed as Equation (4). Note that it is not a chemical equilibrium.

**H₂SO₄**
Optimized initial structure
$E_1$= -700.002134 a.u.
**1**

**H⁺ + HSO₄⁻**
Optimized product structure after H₂SO₄ proton dissociation
$E_1*$= -699.767104 a.u.
**2**

**O₂N-OH₂⁺**
An σ-complex structure setting from
HNO₃ hydroxyl oxygen protonation
**3**

**NO₂⁺ + H₂O**
Optimized structure of 3
$E_1$ = -281.154120 a.u.
**4**

**HOMO**
**NO₂⁺ + H₂O**
An optimized setting structure
$E_{HOMO}$ = -0.506407 a.u.
$E'$= -281.143602 a.u.
**5**

**LUMO**
**NO₂⁺ + H₂O**
An optimized setting structure
$E_{LOMO}$ = -0.073079 a.u.
$E'$= -281.143602 a.u.
**6**

**Figure 1. 1** is the optimized structure of H₂SO₄. **2** is the optimized product structure after H₂SO₄ proton dissociation. **3** is an initial structure setting of HNO₃ hydroxyl oxygen protonation; **4** is an optimized structure of **3** and energy $E_1$. **5** and **6** are an optimized structure setting of NO₂⁺ + H₂O with HOMO and LUMO images and energy $E'$. The solvent is HCONH₂. In **2**, -O⁻···H⁺ = 3.500 Å; In **5** and **6**, H₂O···NO₂⁺ = 2.000 Å, the Chem3D orbital iso-contour = 0.05.

**H₂SO₄ + 3H₂O**
Optimized initial structure setting
$E_1$ = -929.160929 a.u.
**1**

**HSO₄⁻ + H₃O⁺ + 2H₂O**
Optimized product structure
$E_p$ = -929.179383 a.u.
**2**

**H₂SO₄ + H₂O**
Optimized initial structure
$E_1$ = -776.397913 a.u.
**3**

**HSO₄⁻ + H₃O⁺**
Optimized product structure after Lewis collision
$E_p$ = -776.354076 a.u.
**4**
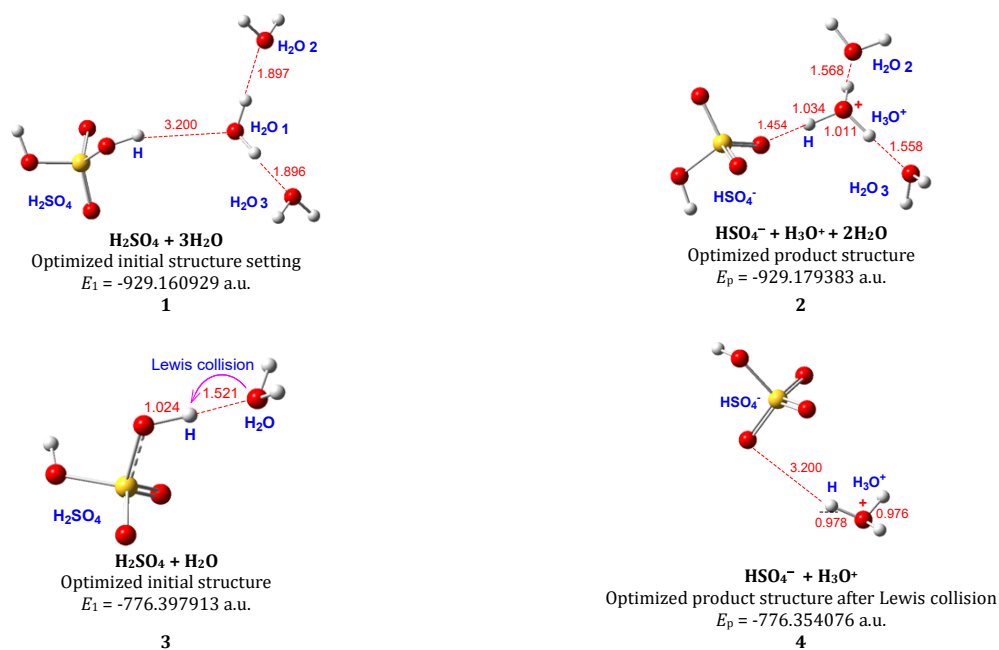
**Figure 2.** The systems **1** and **2** are the formation of H₃O⁺ in water by H₂SO₄ + 3H₂O. The systems **3** and **4** are H₂SO₄ and H₂O in mixed acid by Lewis collision to generate H₃O⁺. The systems **1** and **2**, H₂O as solvent. The systems **3** and **4**, HCONH₂ as solvent. The atom coordinates of structures **1**-**4** see the Supplementary material, S1.

**Lewis collision**

$$H_2SO_4 \;+\; H_2\ddot{O} \quad \xrightleftharpoons[\text{Spontaneous}]{E_a \; 27 \text{ kcal/mol}} \quad HSO_4^- \;+\; H_3O^+ \tag{5}$$

**Lewis acid-base neutralization**
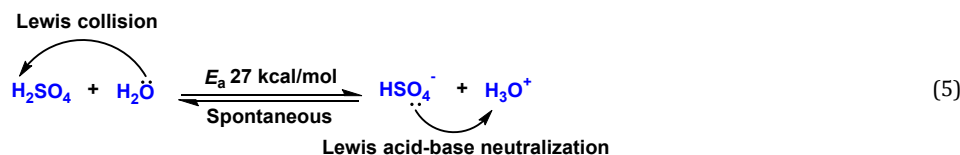
Even in water, if $H_2SO_4$ molecules only interact with one or two $H_2O$ molecules, they cannot spontaneously form $H_3O^+$. Fortunately, $H_2O$ molecules are everywhere in water.

The state of $H_2SO_4$ in mixed acid is completely different from that of water. The **3** in Scheme 2 gives a chemical equilibrium for the formation of $H_3O^+$, but the authors [1,4,5] do not take into account that the $H_2SO_4$ molecule is in mixed acid and is not in water.

For the nitration in mixed acid, usually $HNO_3:H_2SO_4 = 1:2-4$. If the ratio is 1:2, and the nitric acid is with 30% water, it is easy to calculate that ten $H_2SO_4$ molecules in the mixed acid can only get eight $H_2O$ molecules to complex with them, that is, on average, one $H_2SO_4$ molecule cannot get one $H_2O$ molecule to complex. This makes the formed $NO_2^+$ difficult to be acidified by $H_2O$ molecules, which increases the lifetime of $NO_2^+$. Therefore, $NO_2^+$ is easy to survive in mixed acid. A potential energy surface scan (PES) calculation can show that in mixed acid the $NO_2^+$ and $H_3O^+$ can only be generated by a Lewis collision between $H_2SO_4$ and $H_2O$ molecules.

The **3** is the optimized complex structure of $H_2SO_4 + H_2O$ (Figure 2). The distance between the hydroxyl H of $H_2SO_4$ and the O of $H_2O$ is 1.521 Å, and thus it is a strong complex. The **4** is the product structure after the Lewis collision. It is an Opt = Modredundant calculation under freezing coordinates ($HOSO_3^- \cdots H_3O^+ = 3.200$ Å), because there is no the stable product structure of $H_3O^+ + HSO_4^-$. From Figure 2, the **3** and **4**, $E_a = E_p - E_1 = 0.043837$ a.u. = 27.4 kcal/mol, is a high barrier. The chemical Equilibrium (3) in Scheme 2 can be expressed as Equation (5).

Left → right in Equation (5), $H_2SO_4$ and $H_2O$ become into products $H_3O^+ + HSO_4^-$ is through a Lewis collision. It needs to overcome a high barrier 27.4 kcal/mol, which indicates that it is difficult to form $H_3O^+$. The reverse process right → left is a spontaneous bimolecular Lewis acid-base neutralization, indicating that once $H_3O^+$ formed, no matter where it is around $HSO_4^-$, these two will immediately change back to $H_2SO_4$ and $H_2O$, and release the same energy, -27.4 kcal/mole. This shows that the number of $H_3O^+$ in mixed acids is actually zero because it is not a stable intermediate, that is, the chemical equilibrium Step **3** in Scheme 2 does not exist in mixed acid. Therefore, the Step **1** is wrong in Scheme 1. As you will see below, $NO_2^+$ from Lewis collision is different from the $H_3O^+$: it is a stable active intermediate in mixed acid.

### 3.2. Generating active intermediate $NO_2^+$ by Lewis collision

The study shows that the generation of $NO_2^+$ is not through the formation and dissociation of the fictitious σ-complex $H_2O^+$-$NO_2$ (Scheme 2, Steps **1** and **2**). $NO_2^+$ is directly generated by the Lewis collision between a $HNO_3$ and a $H_2SO_4$ or between $2HNO_3$ molecules, but it needs to overcome the highest-barrier in the three-step nitration. Generating $NO_2^+$ by Lewis collision needs to meet three conditions.

First, the collision products must be good leaving groups. The generation of $NO_2^+$ in mixed acid can consider as a $HNO_3$ and a $H_2SO_4$ molecule collide to form a $NO_2^+$, a $H_2O$ and a $HSO_4^-$. These three products are good leaving groups in mixed acid or strong polar solvents. Second, the generation of $NO_2^+$ is through Lewis collision, which does not follow the transition state theory, and thus there is no transition state (TS) barrier in the collision path. A potential energy surface scan calculation shows that there is no transition state barrier along the collision

path of forming $NO_2$. Figure 3 is the optimized initial structure with the collision path (red dotted line) between $HNO_3$ and $H_2SO_4$. This is the most direct and reasonable Lewis collision path. The distance between the H atom of $H_2SO_4$ and the oxygen of the -OH group of $HNO_3$ is 1.870 Å. The optimization result also shows that $HNO_3$ cannot be automatically protonated by $H_2SO_4$ to form water and $NO_2^+$. If the H$\cdots$OH length is $\leqq 1.015$ Å, it will bond to form $H_2O$. Therefore, the interval of the scan is 1.870-1.015 Å. Figure 4 shows the energy curve of the potential energy surface scan (PES). The energy keeps rising with the approach of the distance between the H atom of $H_2SO_4$ and the -OH of $HNO_3$, the energy is the highest at when it reaches 1.015 Å, and is higher 22.0 kcal/mole than that at 1.870 Å. This proves that there is no transition state barrier in the path of Lewis collision. Third, the opt calculation of the product system must show that the $NO_2^+$ from Lewis collision is a stable active intermediate, which ensures that $NO_2^+$ has a measurable concentration in solution. The barrier get by Lewis collision called activation energy $E_a$. Note that if a reaction follows the transition state theory, its barrier is called as the activation barrier, labeled as $\Delta E^*$.

The $E_a$ calculation only requires the energies of optimized initial structure and optimized product structure before and after collision of $HNO_3$ and $H_2SO_4$, but without having to consider how the collision proceeds [38]. The initial structure of the two molecules with the lowest energy before collision is generally easy to determine. However, the product structure after collision is often difficult to do because there are many different product configurations after collision, which needs to find the product system that $NO_2^+$ is a stable intermediate.

The **1** is the optimized initial structure and the energy $E_1$ of $HNO_3 + H_2SO_4$ before collision (Figure 5); **2** is the optimized product structure and energy $E_1^*$ after collision (Figure 5). For the optimized product **2**, here $H_2O$ and $HSO_4^-$ are on both sides of $NO_2^+$, and $NO_2^+$ has good linearity, $\angle ON^+O = 176.7°$. This is an Opt calculation, the three are a stable product system, that is, the $NO_2^+$ is an independent and stable active intermediate. Of course, $\angle ON^+O \neq 180°$ showing that there is a weak electrostatic interaction between the three, but this is normal in solution.

The energy $E_1^*$ of product **2** is higher than the energy $E_1$ of initial structure **1** (Figure 5). The elevated energy is the $E_a$ of forming $NO_2^+$, $E_a = E_1^* - E_1 = 0.028058$ a.u. = 17.6 kcal/mol, is not high, but in the three-step nitration of benzene, the barrier is the highest. The barrier obtained by the DFT calculation is consistent with Sheats' experimental $E_a$ of toluene 18.3±4 kcal/mol [22]. Note that the structure of Figure 3 cannot be used for the initial structure, because the bimolecular system does not have the lowest energy; it is 2.8 kcal/mole higher than that of **1** (Figure 5). The calculation of $E_a$ must use the **1** initial structure with the lowest energy (Figure 5).

Based on the barrier and the stability of $NO_2^+$, $[NO_2^+]$ is high at 50-60 °C, that is, $NO_2^+$ is a measurably stable intermediate. Therefore, the Lewis collision reaction in Figure 5 can be expressed as Equation (6), a chemical equilibrium.

Left → right shows that a $H_2SO_4$ and a $HNO_3$ molecule become to products $NO_2^+ + H_2O + HSO_4^-$ through a Lewis collision, which makes a bimolecular system becomes a tri-molecular one, later will prove that right → left is $NO_2^+$ to be acidified back to $HNO_3$ and $H_2SO_4$, which is a spontaneous tri-molecular electrophilic substitution, $NO_2^+$ is the electrophile, and thus there is no reverse barrier in the equilibrium.

**HNO₃ + H₂SO₄**
An optimized initial structure with a Lewis collision path
$E_1$ = -980.777551 a.u.
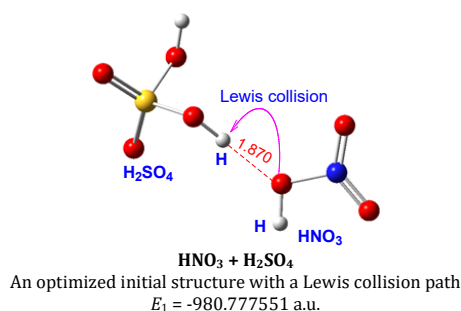
**Figure 3.** An optimized structure of H₂SO₄ and HNO₃ with a Lewis collision path (red dotted line).
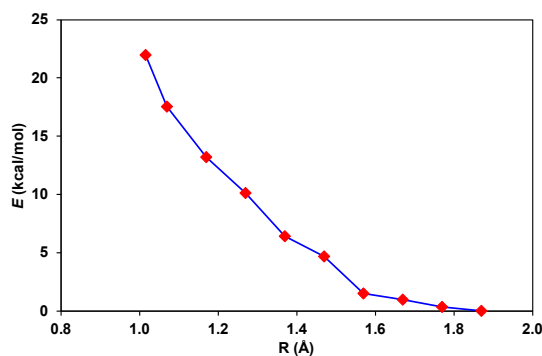


**Figure 4.** The potential energy surface scan curve along the collision path R (HO₃SOH⋯O(H)NO₂).



**HNO₃ + H₂SO₄**
Optimized initial structure
$E_1$ = -980.780930 a.u.
**1**

**NO₂⁺ + H₂O + HSO₄⁻**
Optimized product structure after an effective collision
$E_1$* = -980.752872
**2**
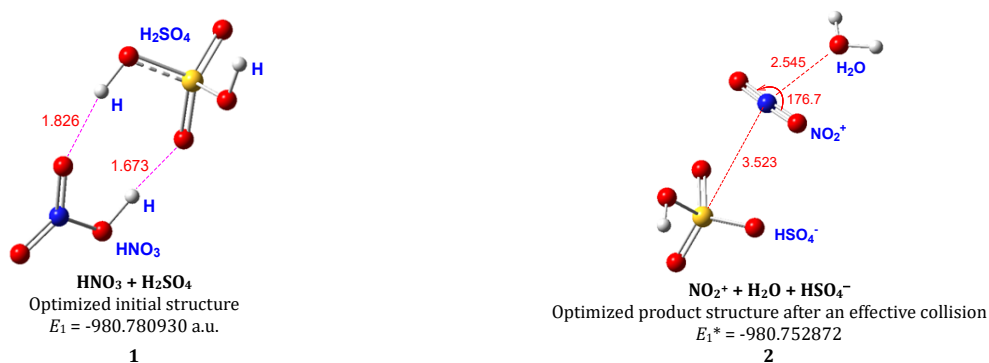
**Figure 5.** Generating NO₂⁺ by Lewis collision of HNO₃ and H₂SO₄ in mixed acid. **1** is the optimized initial structure and energy $E_1$; **2** is the optimized product structure and energy $E_1$* after an effective collision obtained by DFT calculation at the LC-wHPBE/6-311++G(d,p) level. The solvent is HCONH₂. The atom coordinate tables of structures **1** and **2** are presented in the Supplementary material, S2.



$$\text{HO-NO}_2 + \text{HO-SO}_3\text{H} \rightleftharpoons \text{NO}_2^+ + \text{H}_2\text{O} + \text{HSO}_4^- \tag{6}$$

However, although the reverse reaction is spontaneous, the ternary molecule system in Figure 5, **2** takes quite a long time to form an effective tri-molecular acidification system, which gives NO₂⁺ a considerable lifetime, that is, it can form a measurable [NO₂⁺] in the H₂SO₄ + HNO₃ solution. Therefore, Equation (6) is a good chemical equilibrium.

Generating NO₂⁺ in nitric acid also occurs through the Lewis collision between two HNO₃ molecules. The **1** is the optimized initial structure and energy $E_1$ of 2HNO₃ before collision (Figure 6), **2** is the optimized product structure and energy $E_1$* after collision (Figure 6). The optimized product structure **2** also is a stable opt structure, but different from the collision product structure between HNO₃ and H₂SO₄ (Figures 5), the products

H₂O and NO₃⁻ are on the same side of NO₂⁺ and are close to each other. Due to such a configuration, the three are easy to form a tri-molecular acidification system (See Section **3.3**, Figure 7, **5**). The ∠ON⁺O = 173.2°, showing that the NO₂⁺ linearity is worse than that in mixed acid. Therefore, the stability of NO₂⁺ in nitric acid is not as good as in mixed acid.

From Figure 6, the **1** and **2**, $E_a$ = $E_1$* - $E_1$ = 0.034431 a.u. = 21.6 kcal/mol, showing that the collision between the 2 HNO₃ needs to overcome a much higher barrier $E_a$ than the HNO₃ + H₂SO₄ in mixed acid. The Lewis collision reaction in Figure 6 can be expressed as Equation (7).

**HNO₃ + HNO₃**
Optimized initial structure
$E_1$ = -561.563639 a.u.
**1**



**NO₂⁺ + H₂O + NO₃⁻**
Optimized product structure after an effective collision
$E_1^*$ = -561.529208 a.u.
**2**
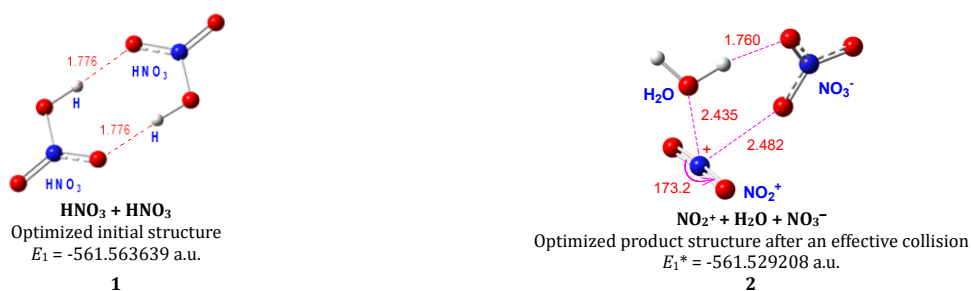
**Figure 6.** Generating $NO_2^+$ by Lewis collision between two $HNO_3$ molecules: **1** is the optimized initial structure and energy $E_1$ of 2 $HNO_3$ before collision; **2** is optimized product structure and energy $E_1^*$ after collision. The solvent is $HCONH_2$. The atom coordinate tables of structures **1** and **2** are presented in the Supplementary material, S3.



(7)
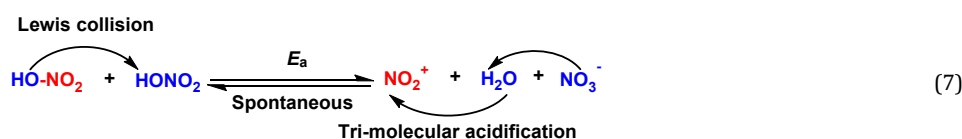
Equation (7) also is a chemical equilibrium [47], the left → right shows that the two $HNO_3$ molecules become into the product $NO_2^+ + H_2O + NO_3^-$ through a Lewis collision, and that makes the bimolecular system becomes a tri-molecular one, but the $E_a$ is much higher than in mixed acid. The right → left is the $NO_2^+$ to be acidified into 2 $HNO_3$, which is a spontaneous tri-molecular electrophilic substitution. Due to the fact that $NO_2^+$ is not an adequate stable ion in nitric acid, the rate at which $NO_2^+$ is acidified is much faster than in mixed acid. Therefore, the $[NO_2^+]$ is much lower than that in mixed acid. Although Equation (7) is a chemical equilibrium, it is not a good one.

The $E_a$ of generating $NO_2^+$ is 21.6 kcal/mol, which is 4 kcal/mol higher than in mixed acid. This is a big increase for reaction barrier. Ingold [15,16] referred to the generation of $NO_2^+$ in nitric acid as an automatic "*self-dissociation*" of $2HNO_3$ molecules. However, the "*self-dissociation*" is not only incorrect, but also needs to overcome a barrier much higher than in mixed acid.

### 3.3. Acidification of NO₂⁺ is a spontaneous poly(≥3)-molecular electrophilic substitution

The DFT calculation found that the nitronium ion $NO_2^+$ is easily acidified back to the $HNO_3$ molecule. The system in mixed acid is a tri-molecular one $NO_2^+ + H_2O + HSO_4^-$ (Equation (6), right → left). A similar tri-molecular system $NO_2^+ + H_2O + NO_3^-$ (Equation (7), right → left) also exists in pure nitric acid. For the benzene nitration in nitric acid, the acidification system $NO_2^+ + nH_2O$ ($n ≥ 2$) also exists because there are large amount of water in nitric acid. The acidification is a spontaneous poly(≥3)-molecular electrophilic substitution. $NO_2^+$ ion is the electrophile. The $HSO_4^-$ or $NO_3^-$ or $H_2O$ is the proton acceptor.

It is generally believed that $NO_2^+$ is acidified through a two-step reaction: $NO_2^+ + H_2O → O_2N-OH_2^+ + H_2O → HONO_2 + H_3O^+$, but the two-step acidification is incorrect. As mentioned above (Section **3.1**), the $NO_2^+$ and one $H_2O$ molecule cannot form the σ-complex (Figure 1, **3**-**6**).

**1** shows an initial tri-molecular structure setting of $NO_2^+ + H_2O + HSO_4^-$ (Figure 7), **2** is the optimized structure of **1**, the optimization generates a $HNO_3$ and a $H_2SO_4$ molecule (Figure 7). In the tri-molecular acidification, $NO_2^+$ combines with the $H_2O$ at the same time the $HSO_4^-$ ion accepted a proton $H^+$ of the $H_2O$, and thus a $H_2SO_4$ and a $HNO_3$ are formed. **1** → **2** is the reverse reaction in Equation (6).

The electrophilic substitution process for acidification of $NO_2^+$ is also the transfer of frontier MO electrons of $H_2O$ to LUMO of $NO_2^+$. $NO_2^+$ and $HSO_4^-$ are acidified to $HNO_3$ and $H_2SO_4$

in one step. The products **3** and **4** are the optimized structure of the setting **1** with HOMO-3 and LUMO images and energy $E'$ (Figure 7). This also is an Opt = Modredundant calculation under freezing coordinates ($H_2O···NO_2^+$ = 2.661 Å). Since $HSO_4^-$ is a negative ion, the HOMO, HOMO-1 and HOMO-2 are all on it, so the frontier MOs of the optimized tri-molecular system are the HOMO-3 on $H_2O$ and LUMO on $NO_2^+$. The orbital symmetry of HOMO-3 (+*) and LUMO (+*) matches, and thus the electron transfer HOMO-3 → LUMO can proceed. Similarly, **5** is an initial tri-molecular structure setting of $NO_2^+ + H_2O + NO_3^-$, **6** is the optimized structure of **5**, showing that the optimization spontaneously generates two $HNO_3$ molecules (Figure 7).

The electron transfer process of the tri-molecular acidification of $NO_2^+ + H_2O + NO_3$ is similar to $NO_2^+ + H_2O + HSO_4^-$ (Figure 7, **3** and **4**) in mixed acid. However, in nitric acid, there is 30-35% water. $NO_2^+ + nH_2O$ ($n ≥ 2$) is also easy to come back $HNO_3$.

$NO_2^+ + 2H_2O$ also is a tri-molecular electrophilic substitution and follows transition state theory, it is not a spontaneous reaction. This is because $HSO_4^-$, $NO_3^-$ are strong Lewis alkali, but $H_2O$ is weak one. **1** and **2** are the optimized initial structure with HOMO and LUMO and energy $E_1$ (Figure 8). The orbital symmetry of the HOMO ($p$ orbital "+*", "-*" of $H_2O$ 1, Figure 8) and the LUMO ($p$ orbital "+*", "-*" of the N atom) in $NO_2^+$ is compatible. Therefore, the HOMO electrons of $H_2O$ 1 (Figure 8) can be transferred to the LUMO of $NO_2^+$.

The **3** is the transition state TS structure with HOMO-1 image, here a small amount of HOMO electrons has transferred to the two oxygen atoms of $NO_2^+$ (see inside curly brackets) (Figure 8). Note that this is a tri-molecular reaction; the pair of HOMO electrons of $H_2O$ (Figure 8) in **1** is not always in the HOMO orbital of thr reaction system during the electron transfer process. In the TS, the frontier MO electron of $H_2O$ 1 (Figure 8) is now in the HOMO-1 (HOMO is not given here). From **1** and **3**, $\Delta E^*$ = 0.009029 a.u. = 5.7 kcal/mol (Figure 8). The barrier is low, so the electron transfer is similar to be a spontaneous process.

**4** is the optimized product structure with HOMO image of the tri-molecular acidification (Figure 8). The $H_2O$ 1 in Figure 8 has completed the electron transfer and $HNO_3$ has been generated. At the same time, the $H_2O$ 2 (Figure 8) molecule accepts the proton of $H_2O$ 1, the $H_3O^+$ ion has been generated, and thus the tri-molecular electrophilic substitution is completed.
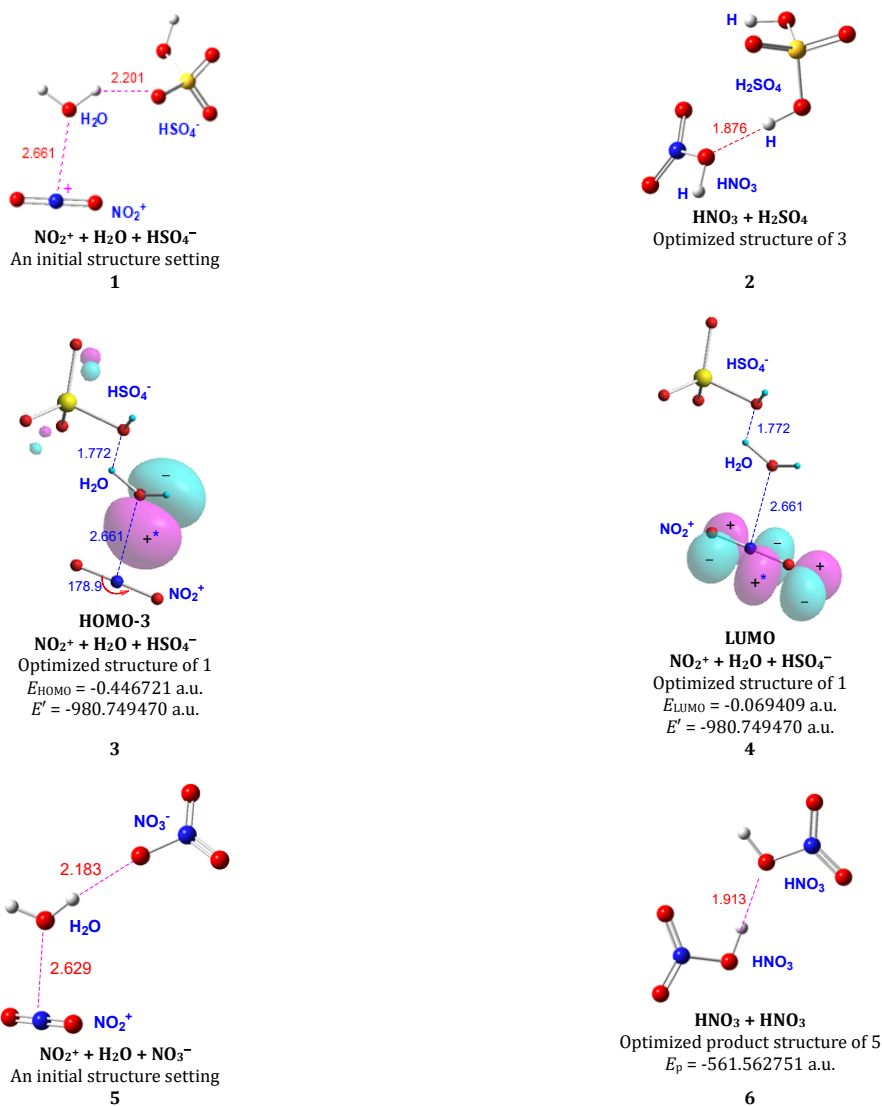
**Figure 7.** Products **1** and **5** are an initial tri-molecular structure setting of $NO_2^+ + H_2O + HSO_4^-$ and $NO_2^+ + H_2O + NO_3^-$. Products **2** and **6** are the optimized product structures of **1** and **5**. Products **3** and **4** are the optimized initial structure setting of **1** with HOMO-3 and LUMO images and energy $E'$ under freezing coordinates $H_2O \cdots NO_2^+ = 2.661$ Å. The solvent is $HCONH_2$. Chem3D Orbital iso-contour = 0.05.

The DFT calculation shows that if the acidification of $NO_2^+$ is carried out under the action of $2\text{-}5H_2O$ molecules, it needs to overcome a barrier of 1-6 kcal/mol. The barriers are very low, and thus they are an approximately spontaneous reaction. The study found that if $NO_2^+$ is to spontaneously complete the acidification by water, at least six $H_2O$ molecules must participate in the reaction. The **1** is an initial structure setting of $NO_2^+ + 6H_2O$, a seven molecular reaction system (Figure 9). The product **2** is the optimized product structure of **1** (Figure 9).

The acidification of $NO_2^+$ in Figure 9 is a spontaneous seven-molecular electrophilic substitution [38]. The products are $HNO_3$ and $H_3O^+$. The four $H_2O$ molecules, $H_2O$ and $H_2O$ 4-6 played a catalytic role in the reaction. Of course, such a spontaneous seven-molecular acidification is completely impossible in mixed acids. It is estimated that even in nitric acid, the chance of occurrence also is extremely small.

In mixed acid, although $[H_2O]$ is greatly reduced, there is a content of ~10%. The tri-molecular acidification (Figure 7, **1→2**) is spontaneous and fast, and thus the benzene nitration often maintains at 50-60 °C and under effective stirring. This can increase $[NO_2^+]$, and enables that once $NO_2^+$ is formed, benzene molecules can be nitrated immediately.

Nitric acid contains 30-35% water, which is very high. The molecular weight of $HNO_3$ is 3.5 times that of $H_2O$, that is, the mole amount of $H_2O$ in nitric acid is about 1.5 times that of $HNO_3$. Therefore, in nitric acid, there is not only an acidification path of $NO_2^+ + H_2O + NO_3^-$, but also $NO_2^+$ can be quickly acidified by water, and therefore $[NO_2^+]$ in nitric acid is extremely low. It is inevitable that the nitration of benzene is difficult to perform in nitric acid.

### 3.4. Generating σ-complex intermediate by electrophilic addition of $C_6H_6$ and $NO_2^+$

The DFT calculation shows that the electrophilic addition of $NO_2^+$ and $C_6H_6$ generate an σ-complex intermediate, it follows the transition state theory, and need to overcome a low activation barrier $\Delta E^*$. $NO_2^+$ is the electrophile. **1** and **2** show the optimized initial structure with HOMO and HOMO-1 of $C_6H_6$ and energy $E_1$ (Figure 10). The HOMO and HOMO-1 are two degenerate orbitals. The orbital energy difference of HOMO and HOMO-1 is $\Delta E_{HH-1} = 0.03$ eV, is very small, and thus HOMO-1 is also a frontier MO (Figure 10). **3** is the optimized initial structure with LUMO image of $NO_2^+$ (Figure 10). Note that the LUMO and LUMO+1 of $NO_2^+$ both are approximately the degenerate
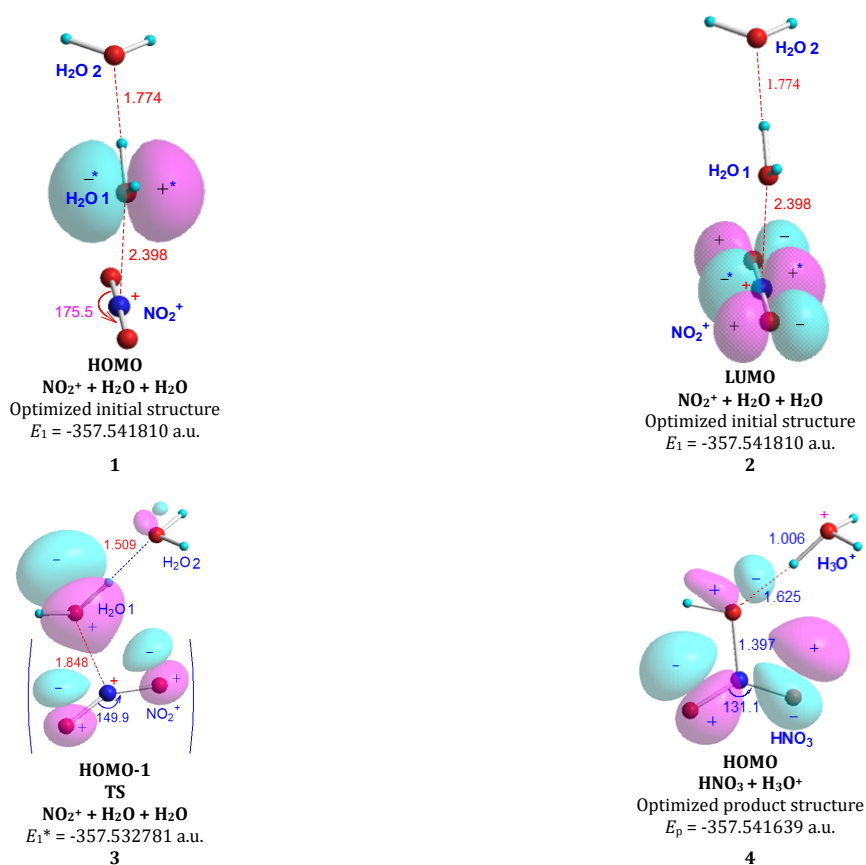
**Figure 8.** The systems **1** and **2** are the optimized initial structure with HOMO and LUMO images, and Energy $E_1$ of $NO_2^+$ + $2H_2O$ system. **3** is the transition state TS with HOMO -1 and energy $E_1^*$, **4** is the optimized product structure with HOMO images and energy $E_p$. Chem3D, Orbital iso-contour = 0.05. The solvent is $HCONH_2$. The coordinate tables of structures **1-4** see Supplementary material, S4.
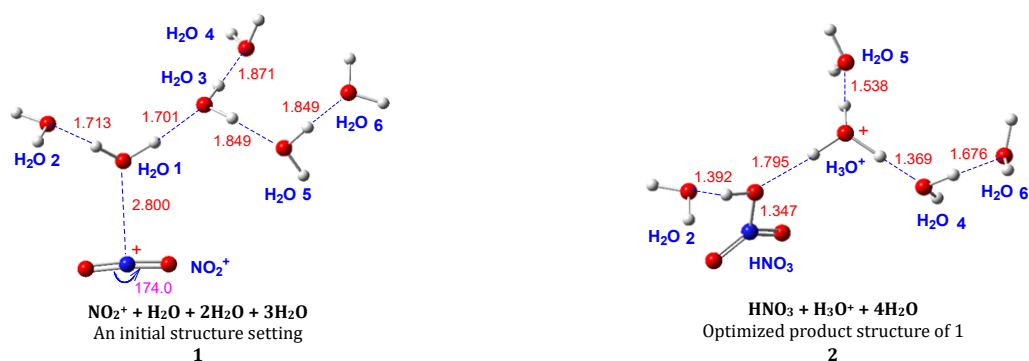


**Figure 9.** The acidification of $NO_2^+$ + $6H_2O$ is a spontaneous seven-molecular electrophilic substitution. **1** is the initial structure setting of the seven-molecular system. **2** is the optimized product structures of **1**.

orbitals ($\Delta E_{LL+1}$ = 0.01 eV). Therefore, LUMO+1 is also a frontier MO. However, the LUMO+1 and the HOMO or HOMO-1 do not match, so the optimized initial structure with the LUMO+1 image is not shown.

The $C_6H_6$ + $NO_2^+$ is an electrophilic addition between both. The essence of the addition is the transfer of HOMO-1 electrons of $C_6H_6$ in **2** to the LUMO orbital of $NO_2^+$ in **3** (Figure 10). From **2** and **3**, the orbital symmetry of the HOMO-1 (+*, -*) of $C_6H_6$ and the LUMO (+*, -*) of $NO_2^+$ matches (Figure 10). Therefore, the HOMO-1 electrons of $C_6H_6$ can transfer to the LUMO of $NO_2^+$.

**4** is the transition state (TS) structure with the HOMO image and the energy $E_1^*$ (Figure 10). The C⋯$NO_2^+$ distance is 2.261 Å (Figure 10). The transfer of HOMO electrons of $C_6H_6$ in TS to the LUMO of $NO_2^+$ does not appear. This is the inevitable result of the symmetry mismatch between **1** and **3**.

**5** is the TS structure with HOMO-1 image. In the TS, many HOMO-1 electrons of $C_6H_6$ have transferred to the C- - $NO_2^+$ region (see inside blue braces). This is also the inevitable result of the symmetry match between **2** and **3**. **4** and **5** indicate that the symmetry matching between two frontier MOs is a necessary condition for the realization of electron transfer. It can be seen from Figure 10 **2**, **3** and **5**, the frontier MOs electron-transfer of the electrophilic addition is HOMO-1 **2** → LUMO **3**.

From the initial structure energy $E_1$ and the energy $E_1^*$ of TS, the activity barrier of $NO_2^+$ and $C_6H_6$ electrophilic addition $\Delta E_1^* = E_1 – E_1^*$ = 0.010975 a.u = 6.7 kcal/mol (Figure 10). The barrier ($HCONH_2$ as solvent) is consistent with Sheats's [22] two barriers 5.9±0.1 and 6.3±0.5 kcal/mol of the generated toluene σ-complex.

**Table 1.** The optimized initial energy $E_I$, the TS energy $E_1*$, the optimized σ-complex energy $E_σ$, activation barrier $\Delta E*$, reverse barrier $\Delta E_r*$ and the reaction heat $\Delta H_σ$ of generating σ-complex in HCONH$_2$ obtained by DFT calculation at the LC-wHPBE, M06-2x, M05-2x/6-311++G(d,p) level.

| DFT method | $E_1$ (a.u.) | $E_1*$ (a.u.) | $E_σ$ (a.u.) | $\Delta E*$ | $\Delta E_r*$ | $\Delta H_σ$ (kcal/mol) |
|---|---|---|---|---|---|---|
| LC-wHPBE | -436.701413 | -436.690750 | -436.717861 | 6.7 | 17.0 | -10.3 |
| M06-2x | -436.820069 | -436.815555 | -436.838644 | 2.8 | 14.5 | -11.7 |
| M05-2x | -436.937376 | -436.935834 | -436.959364 | 1.1 | 14.8 | -13.8 |
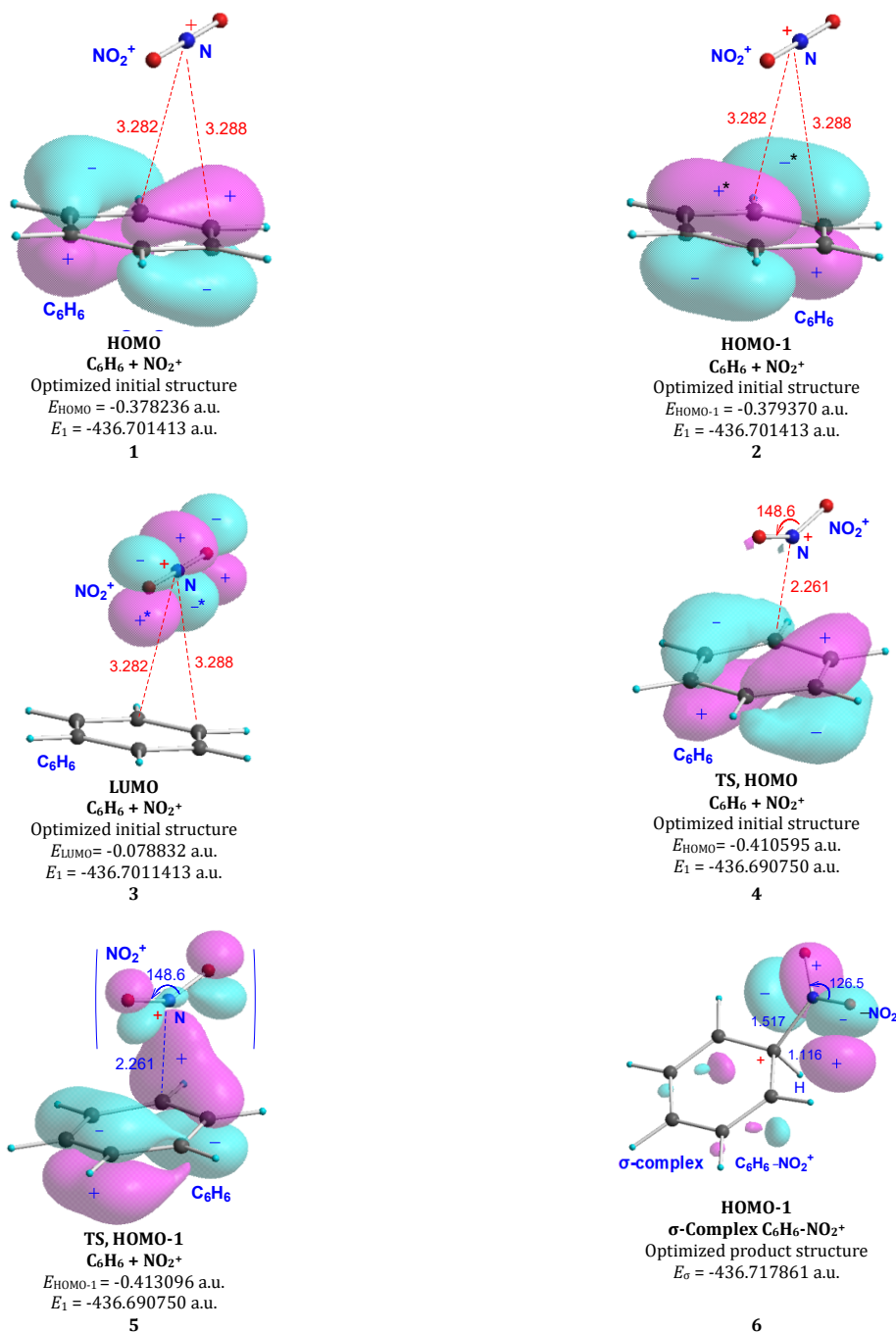


**Figure 10.** The **1**, **2** and **3** are the optimized initial structure with HOMO, HOMO-1 and LUMO, and system energy $E_1$; **4** and **5** are the transition state TS structure with HOMO, HOMO-1 images and energy $E_1*$. **6** is an optimized product structure with HOMO-1 and energy $E_σ$. Orbital iso-contour = 0.04. The bond distance is in Å. Angle is in degree. The solvent is HCONH$_2$. The atom coordinate tables of structures **1-6** see the Supplementary material, S5.

It is reasonable that toluene has a lower barrier of generating σ-complex than benzene, because toluene has a higher reactivity than benzene.

The **6** is the optimized product structure with the HOMO-1 image and energy $E_σ$ (Figure 10). The σ-complex of C$_6$H$_6$ + NO$_2^+$ has been generated. The σ-C-NO$_2^+$ bond is 1.517 Å. At this time, almost all HOMO-1 electrons have transferred to the σ-C-NO$_2$ area. This further shows that the essence of the electrophilic addition is the transfer of HOMO-1 electrons of C$_6$H$_6$ to LUMO of NO$_2^+$. From **2** and **6**, the reaction heat is $\Delta H_σ = E_σ - E_1 = -0.016448$ a.u. = -10.3 kcal/mol, showing that the σ-complex is a stable intermediate (Figure 10). Since the electrophilic addition of NO$_2^+$ + C$_6$H$_6$ follows the transition state theory, there is an inverse barrier $\Delta E_r*$ for the addition.

**Table 2.** The optimized initial structure energy $E_1$, optimized product structure energy $E_p$, and released reaction heat $\Delta H_p$ of generating final products of σ-$C_6H_6$-$NO_2^+$ + $HSO_4^-$ or + $NO_3^-$ or + $H_2O$ in $HCONH_2$.

| Reaction | $E_1$ (a.u.) | $E_p$ (a.u.) | $\Delta H_p$ (kcal/mol) |
|---|---|---|---|
| $1 \rightarrow 2$ σ-$C_6H_6$-$NO_2^+$ + $HSO_4^-$ → $C_6H_5NO_2$ + $H_2SO_4$ (Figure 11) | -1136.310969 | -1136.380100 | -43.4 |
| $3 \rightarrow 4$ σ-$C_6H_6$-$NO_2^+$ + $NO_3^-$ → $C_6H_5NO_2$ + $HNO_3$ (Figure 11) | -717.088022 | -717.167531 | -49.9 |
| $5 \rightarrow 6$ σ-$C_6H_6$-$NO_2^+$ + $H_2O$ → $C_6H_5NO_2$ + $H_3O^+$ (Figure 11) | -513.105180 | -513.140748 | -22.3 |

**Table 3.** $E_a$, $\Delta H_\sigma$, and $\Delta H_p$ (here take the integer according to rounding after the decimal point) and total reaction heat $\Delta H$ of benzene nitration obtained by DFT calculation at the LC-wHPBE/6-311++G(d,p) level. $HCONH_2$ as solvent.

| Nitration solvent | $E_a$ | $\Delta H_\sigma$ | $\Delta H_p$ | $\Delta H$ (kcal/mole) |
|---|---|---|---|---|
| Mixed acid | 18 | -10 | -43 | **-35** |
| Nitric acid | 22 | -10 | -50 | **-38** |

From **5** and **6**, $\Delta E_r^* = 0.027111$ a.u. = 17.0 kcal/mol (Figure 10). Sheats [22] gave the reverse activation energy of toluene generating $NO_2^+$ to be 10.5 or 12.0±4.0 kcal/mol. The barrier is consistent with the inverse barrier 17.0 kcal/mol for $C_6H_6$ + $NO_2^+$. This is because Sheats's detection method cannot deter-mine whether the reaction follows the transition state theory or is through Lewis collision, so he cannot determine the reverse barrier should attribute to the $\Delta E_r^*$ of toluene generating σ-complex.

Table 1 lists the activation barriers $\Delta E^*$ and the reaction heat $\Delta H_\sigma$ of the forming σ-complex obtained by the DFT calculation at the LC-wHPBE/6-311++G(d,p) level. The barrier is consistent with the experimental data [22]. The reaction heat $\Delta H_\sigma$ from the DFT calculation are -10.3 kcal/mol, showing that the σ-complex is a stable intermediate. The $\Delta H_\sigma$ is closer to the experimental value (-7.4 kcal/mol) than that (-13.0 kcal/mol) of Brinck group [33].

Table 1 also presents the results of the DFT calculation at the M06-2x and M05-2x/6-311++G(d,p) level [48]. Clearly, the barriers $\Delta E^*$ of generating σ-complex of $C_6H_6$ + $NO_2^+$ are much lower than those obtained by LC-wHPBE, but the released reaction heats $\Delta H_\sigma$ are much larger than those obtained by LC-wHPBE. These $\Delta E^*$, $\Delta E_r^*$, and $\Delta H_\sigma$ data are greatly deviated from the experimental results [22]. Especially the results of M05-2x are the worst.

Furthermore, if the old functional B3LYP or B3P86 or B3PW91 is used in the DFT calculation, the $C_6H_6$ + $NO_2^+$ addition is spontaneous without any barrier, the result is highly inconsistent with the experiment [22]. Therefore, these old functionals are more than not suitable for the study of the mechanism of benzene nitration. In fact, the LC-wHPBE functional is the best for mechanism research [36].

### 3.5. Last Step 3 of benzene nitration is a spontaneous Lewis acid-alkali neutralization

The DFT calculations found that the σ-complex $C_6H_6$-$NO_2^+$ can complete the last Step **3** (Scheme 1) with the $HSO_4^-$ or $NO_3^-$ ions or the $H_2O$ molecule through a spontaneous Lewis acid-base neutralization, and release a lot of heat. That is, Step **3** in Scheme 1 of generating product nitrobenzene is a spontaneous reaction and does not need to overcome any barrier.

The **1**, **3**, and **5** show the optimized initial structures of σ-$C_6H_6$-$NO_2^+$ + $HSO_4^-$ or + $NO_3^-$ or + $H_2O$ (Figure 11). The $HSO_4^-$ or $NO_3^-$ or $H_2O$ definitely is on the side of σ-$C_6H_6$-$NO_2^+$, which can ensure that it is a stable initial structure. There is considerable electrostatic interaction between the positive and negative two ions. It is important to include the energy of the interaction between the two ions to correctly calculate the reaction heat of Step **3** (Scheme 1). The **2**, **4** and **6** show the optimized product structures of σ-$C_6H_6$-$NO_2^+$ + $HSO_4^-$ or + $NO_3^-$ or + $H_2O$ (Figure 11). The product nitrobenzene $C_6H_5$-$NO_2$ + $H_2SO_4$ or + $HNO_3$ or + $H_3O^+$ all generated, showing that the nitration reaction has ended.

The optimized initial system energies $E_I$, optimized product energy $E_p$, and released reaction heat $\Delta H_p$ of $1 \rightarrow 2$, $3 \rightarrow 4$ and $5 \rightarrow 6$ (Figure 11) are listed in Table 2.

From Table 2, the $1 \rightarrow 2$ and $3 \rightarrow 4$ are a strongly exothermic reaction, the heats are -43.4 and -49.9 kcal/mole (Figure 11). The reason for releasing so much heat is that the σ-$C_6H_6$-$NO_2^+$ is a strong Lewis acid, $HSO_4^-$ or $NO_3^-$ is a strong Lewis base, and therefore $1 \rightarrow 2$ and $3 \rightarrow 4$ are a strong acid-base neutralization.

The $5 \rightarrow 6$, $\Delta H_p$ is -22.3 kcal/mol (Figure 11). The heat released is much less than that of $1 \rightarrow 2$ and $3 \rightarrow 4$, which is because $H_2O$ is a neutral molecule, a weak Lewis base. The reaction product is $C_6H_5NO_2$ + $H_3O^+$. The occurrence of $5 \rightarrow 6$ in mixed acids is negligible because even a trace amount of $H_3O^+$ is generated, it will immediately will immediately acid-base neutralize with $HSO_4^-$ to form $H_2SO_4$. However, in nitric acid there will be a considerable amount of occurrence of $5 \rightarrow 6$ because nitric acid contains 30-35% water. Of course, the $H_3O^+$ will also be neutralized by $NO_3^-$ soon.

The total nitration reaction is $C_6H_6$ + $HNO_3$ → $C_6H_5$-$NO_2$ + $H_2O$, which is a strongly exothermic reaction. The experimental reaction heat of benzene nitration in mixed acid is $\Delta H$ = -34 kcal/mol (-142 kJ/mol) [49]. According to the results above, the total nitration reaction heat $\Delta H$ released by the three steps in mixed acid or nitric acid is expressed as Equation (8),

$$\Delta H = E_a + \Delta H_\sigma + \Delta H_p \qquad (8)$$

The $E_a$, $\Delta H_\sigma$, $\Delta H_p$ and $\Delta H$ data of nitration in mixed acid and in nitric acid are given in Table 3.

The released nitration reaction heat in mixed acid is $\Delta H$ = -35 kcal/mol, which is good consistent with the experimental reaction heat $\Delta H$ = -34 kcal/mol. We have not found the experimental reaction heat $\Delta H$ of benzene nitration in nitric acid, and thus lack a comparison with its experimental data. If there is no the experimental result in nitric acid so far, the DFT calculation result can regard as a prediction for the reaction heat $\Delta H$.

### 3.6. A corrected benzene nitration three-step mechanism

Based on the above calculation results, the classic nitration mechanism in mixed acid is corrected as following Scheme 3. The $E_a$, $\Delta H_\sigma$, and $\Delta H_p$ values (Table 3, Scheme 3) are from the DFT calculation results of benzene nitration in $HCONH_2$ with the highest polarity (ε = 108.9; $H_2SO_4$ ε ≅ 100).

Step **1** shows the formation of nitronium ions $NO_2^+$ by Lewis collision of $HNO_3$ and $H_2SO_4$ in mixed acid and the collision needs to overcome a barrier $E_a$ = 18 kcal/mol. The study also shows how to calculate its activation energy $E_a$ for Lewis collision reaction (see Section **3.2**).

Step **2** is the electrophilic addition of $C_6H_6$ + $NO_2^+$, $NO_2^+$ is the electrophile (Scheme 3). The addition follows the transition state theory and needs to overcome a low barrier $\Delta E^*$ = 7 kcal/mol. The product is an σ-complex $C_6H_6$-$NO_2^+$. The activation barrier $\Delta E^*$ of the generating σ-complex also is consistent with Sheats's that obtained by stopped flow spectrometer [22]. Generating σ-complex is an exothermic reaction, $\Delta H_\sigma$ = -10 kcal/mol. Therefore, the σ-complex is a stable intermediate, which agrees with the experimental facts [23].
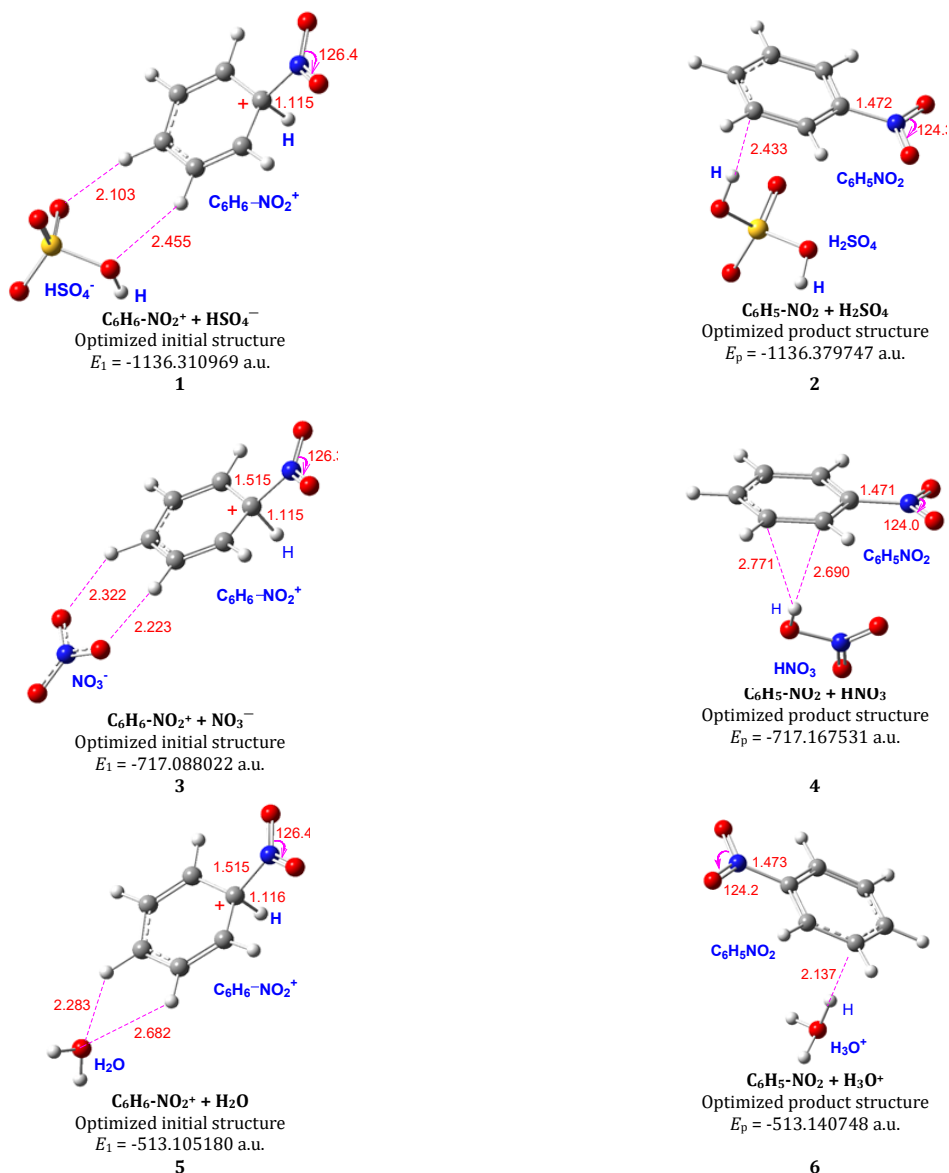
**Figure 11.** Systems **1**, **3** and **5** are the optimized initial structure of σ-C$_6$H$_6$-NO$_2^+$ + HSO$_4^-$ or + NO$_3^-$ or + H$_2$O. Systems **2**, **4**, and **6** are the optimized product structure. The solvent is HCONH$_2$. The bond distance is in Å. Angle is in degree. The atom coordinate tables of **1**-**6** are given in the Supplementary material, S6.
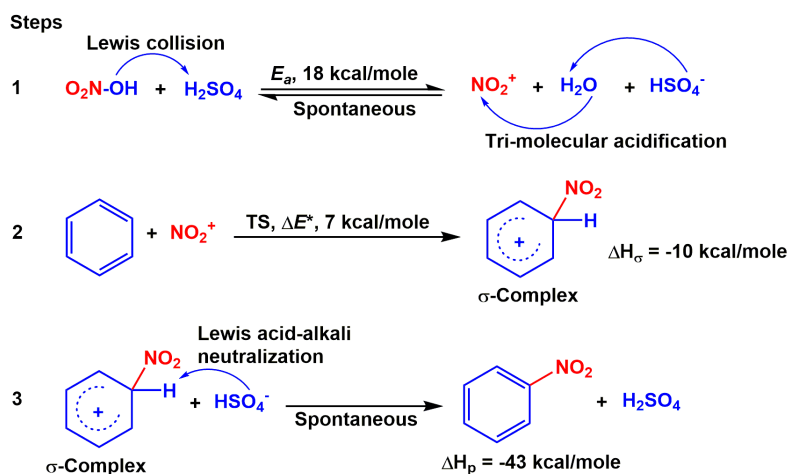


**Scheme 3.** A corrected three-step mechanism of benzene nitration in mixed acid (HNO$_3$ + H$_2$SO$_4$) obtained by DFT calculation at the LC-wHPBE/6-311++G(d,p) level.

The DFT calculation found that the nature of the electrophilic addition of the generated σ-complex is the transfer of the HOMO-1 electrons of $C_6H_6$ to the LUMO of $NO_2^+$. The inverse barrier $\Delta E_r^* = 17$ kcal/mol is much higher than the addition barrier $\Delta E^* = 7$ kcal/mol, and thus Step 2 is not a chemical equilibrium, is a one-way reaction (Scheme 3). Step 3 is a spontaneous Lewis acid-base neutralization, and is a strongly exothermic reaction $\Delta H_p = -43$ kcal/mol, and thus it also is a one-way reaction (Scheme 3). The results of the DFT calculation indicate that the rate control step of benzene nitration is not step 2 of generating σ-complex, but is Step 1 of generating $NO_2^+$ (Scheme 3).

Quantum chemistry calculations can obtain the barrier or reaction heat of each step, but it is impossible to get these data using classical research methods. Chemical kinetic study [15] shows that benzene nitration exhibits second-order kinetics in sulfuric acid, V = $k\times[C_6H_6]\times[HNO_3]$. Step 1 in Scheme 3 shows that the $[NO_2^+]$ is proportional to $[HNO_3]$, and the probability of forming σ-complex is proportional to the reaction probability between $C_6H_6$ and $NO_2^+$, that is, the rate proportional to $[C_6H_6]$ and $[HNO_3]$, which is consistent with the second-order kinetics. In nitric acid, V = $k\times[C_6H_6]$, because $[HNO_3]$ = constant. Therefore, the corrected mechanism in Scheme 3 is consistent with the experimental result [15,16].

In kinetic study of nitration reaction, often by comparing deuterated, tritiated aromatic nitration rate to determine whether the C-H bond of σ-complex is broken in rate-controlling step. Melander's experiment [50] shows that there is no isotopic effect in the nitration of most aromatic compounds including benzene. The nitration of benzene is a three-step reaction, and the first step is a rate-controlling step. Steps 2 and 3 determine whether there is an isotope effect in the nitration (Scheme 3). Step 2 generates the σ-complex, which needs to overcome a barrier (7 kcal/mole), which is a slow ($K_1$) step. Step 3 is to remove the proton, it is a spontaneous Lewis acid-base neutralization, so it is a very fast ($K_2$) step. Hence $K_1 \square K_2$, which is consistent with the Melander's experimental result. The textbook mechanism in Scheme 1 is qualitatively consistent with the experiment, because step 2 and step 3 both need to overcome the barriers, and the rate of step 2 is slow, that of step 3 is fast. However, no one knows how high the two barriers are. Therefore, there is a lack of quantitative comparison on these two barriers.

For Step 3 of the nitration mechanism, some textbooks use $HSO_4^-$ as the proton acceptor [1,2], but the others [3,4] use $H_2O$ as the acceptor. Which one is right, or which one is better? The DFT calculation shows that the correct choice should be $HSO_4^-$ in mixed acid.

## 4. Conclusions

The study shows that in organic chemistry textbooks the benzene nitration mechanism is a three-step reaction, and $NO_2^+$ and σ-complex $C_6H_6NO_2^+$ are the two active intermediates of benzene nitration, which are correct. However, no correct answers are given as to how to generate these two active intermediates and how to complete these three nitration steps. Step 1 of generating $NO_2^+$ is not a spontaneous reaction. Its generation occurs through Lewis collision and must overcome an no-high barrier $E_a = 18$ kcal/mol, but the $NO_2^+$ can return to $HNO_3$ through a spontaneous poly(≥3)-molecular acidification. Step 2 is the electrophilic addition of $NO_2^+ + C_6H_6$. The product is an σ-complex. The addition follows the transition state theory and needs to overcome a much lower barrier $\Delta E_1^* = 7$ kcal/mol than Step 1 of generating $NO_2^+$. The essence of electrophilic addition is the transfer of HOMO-1 electrons of $C_6H_6$ to LUMO of $NO_2^+$. Step 3 is a spontaneous Lewis acid-base neutralization, generates the target product nitrobenzene, and releases a lot of heat $\Delta H_p = -43$ kcal/mol. The final step does not need to

overcome any barrier. Therefore, the rate-controlling step of the benzene nitration is not Step 2 of generating σ-complex, but is step 1 of generating $NO_2^+$ The DFT calculation obtains the total nitration reaction heat $\Delta H = -35$ kcal/mol. It is consistent with the experimental $\Delta H = -34$ kcal/mol, indicating that the corrected benzene nitration three-step mechanism has been experimentally confirmed.

## Supporting information Ⓢ

The atom coordinate tables of reaction structures in Figures. **S1**, Structures **1**-**4** in Figure 2; **S2**, Structures **1** and **2** in Figure 5; **S3**, Structures **1** and **2** in Figure 6; **S4**, Structures **1**-**4** in Figure 8; **S5**, Structures **1**-**6** in Figure 10; **S6**, Structures **1**-**6** in Figure 11.

## Disclosure statement Ⓓⓢ

Conflict of interest: The author declares that he has no conflict of interest. Ethical approval: All ethical guidelines have been adhered.

## CRediT authorship contribution statement Ⓒⓡ

Conceptualization, Methodology, Formal Analysis, Investigation, Data Curation, Writing - Original Draft, Writing - Review and Editing, Visualization, Project Administration: Hongchang Shi. The selection of topic, literature search, DFT calculation, data sorting, structure diagram production, and paper writing were all done by the author.

## ORCID Ⓘⓓ and Email ✉

Hongchang Shi
✉ shihc@mail.tsinghua.edu.cn
Ⓘⓓ https://orcid.org/0000-0001-7505-4976

## References

[1].   Graham Solomons, T. W. *Organic Chemistry*; 6th ed.; John Wiley and Sons (WIE): Brisbane, QLD, Australia, 1995.
[2].   Carey, F. A. *Organic Chemistry*; 2nd ed.; McGraw-Hill: New York, NY, 1992.
[3].   Vollhardt, K. P. C.; Schore, N. *Organic Chemistry*; 2nd ed.; W.H. Freeman: New York, NY, 1993.
[4].   Xing Q. Y.; Pei W. W.; Xu R.; Pei Q. J. *Foundation of Organic Chemistry, Third Edition (Chinese)*; Higher Education Press: Beijing, China, 2005.
[5].   Smith, M. B.; March, J. *March's advanced organic chemistry: Reactions, mechanisms, and structure*; 7th ed.; Wiley-Blackwell: Hoboken, NJ, 2012.
[6].   Carey, F. A.; Sundberg, R. J. *Advanced organic chemistry: Part A: Structure and mechanisms*; 5th ed.; Springer: New York, NY, 2007.
[7].   Euler, H. Zur Kenntniss der aliphatischen Amine. *Justus Liebigs Ann. Chem.* **1904**, *330*, 280–291.
[8].   Westheimer, F. H.; Kharasch, M. S. The kinetics of nitration of aromatic Nitro compounds in sulfuric acid. *J. Am. Chem. Soc.* **1946**, *68*, 1871–1876.
[9].   Bennett, G. M.; Brand, J. C. D.; Williams, G. 188. Nitration in sulphuric acid. Part I. The nature of the nitrating agent in nitric–sulphuric acid mixtures. *J. Chem. Soc.* **1946**, 869–875.
[10].   Olah, G. A. Aromatic substitution. XXVIII. Mechanism of electrophilic aromatic substitutions. *Acc. Chem. Res.* **1971**, *4*, 240–248.
[11].   Ridd, J. H. Mechanism of aromatic nitration. *Acc. Chem. Res.* **1971**, *4*, 248–253.
[12].   Hughes, E. D.; Ingold, C. K.; Reed, R. I. Kinetics of aromatic nitration: The nitronium ion. *Nature* **1946**, *158*, 448–449.
[13].   Hughes, E. D.; Ingold, C. K.; Reed, R. I. 493. Kinetics and mechanism of aromatic nitration. Part II. Nitration by the nitronium ion, NO2 +, derived from nitric acid. *J. Chem. Soc.* **1950**, 2400–2440.
[14].   Gold, V.; Hughes, E. D.; Ingold, C. K.; Williams, G. H. 495. Kinetics and mechanism of aromatic nitration. Part IV. Nitration by dinitrogen pentoxide in aprotic solvents. *J. Chem. Soc.* **1950**, 2452–2466.
[15].   Gold, V.; Hughes, E. D.; Ingold, C. K. 496. Kinetics and mechanism of aromatic nitration. Part V. Nitration by acyl nitrates, particularly by benzoyl nitrate. *J. Chem. Soc.* **1950**, 2467–2473.

[16]. Gillespie, R. J.; Hughes, E. D.; Ingold, C. K. 504. Cryoscopic measurements in nitric acid. Part I. The solutes dinitrogen pentoxide and water. The self-dissociation of nitric acid. *J. Chem. Soc.* **1950**, 2552–2558.

[17]. Ingold, C. K.; Millen, D. J.; Poole, H. G. 506. Vibrational spectra of ionic forms of oxides and oxy-acids of nitrogen. Part I. Raman-spectral evidence of the ionisation of nitric acid by perchloric, sulphuric, and selenic acids. Spectroscopic identification of the nitronium ion, NO2 +. *J. Chem. Soc.* **1950**, 2576–2589.

[18]. Ingold, C. K.; Millen, D. J. 510. Vibrational spectra of ionic forms of oxides and oxy-acids of nitrogen. Part V. Raman spectral evidence of the ionisation of dinitrogen pentoxide in nitric acid, and of the constitution of anhydrous nitric acid. *J. Chem. Soc.* **1950**, 2612–2619.

[19]. Bunton, C. A.; Hughes, E. D.; Ingold, C. K.; Jacobs, D. I. H.; Jones, M. H.; Minkoff, G. J.; Reed, R. I. 512. Kinetics and mechanism of aromatic nitration. Part VI. The nitration of phenols and phenolic ethers: the concomitant dealkylation of phenolic ethers. The role of nitrous acid. *J. Chem. Soc.* **1950**, 2628–2656.

[20]. Ingold, C. K. *Structure and mechanism in organic chemistry*; 2nd ed.; HarperCollins Distribution Services: Glasgow, Scotland, 1970.

[21]. Benford, G. A.; Bunton, C. A.; Halbertstadt, E. S.; Hughes, E. D.; Ingold, C. K.; Minkoff, G. J.; Reed, R. I. Univalent electron transfers in aromatic nitration? *Nature* **1945**, *156*, 688–688.

[22]. Sheats, G. F.; Strachan, A. N. Rates and activation energies of nitronium ion formation and reaction in the nitration of toluene in ~78% sulphuric acid. *Can. J. Chem.* **1978**, *56*, 1280–1283.

[23]. Politzer, P.; Jayasuriya, K.; Sjoberg, P.; Laurence, P. R. Properties of some possible intermediate stages in the nitration of benzene and toluene. *J. Am. Chem. Soc.* **1985**, *107*, 1174–1177.

[24]. Olah, G. A.; Malhotra, R.; Narang, S. C. *Nitration: Methods and mechanisms*; Wiley-Interscience: Newy York, 1989.

[25]. Cardoso, S. P.; Carneiro, J. W. de M. Nitração aromática: substituição eletrofílica ou reação com transferência de elétrons? *Quim. Nova* **2001**, *24*, 381–389.

[26]. Gwaltney, S. R.; Rosokha, S. V.; Head-Gordon, M.; Kochi, J. K. Charge-transfer mechanism for electrophilic aromatic nitration and nitrosation via the convergence of (ab initio) molecular-orbital and Marcus-Hush theories with experiments. *J. Am. Chem. Soc.* **2003**, *125*, 3273–3283.

[27]. Esteves, P. M.; De M Carneiro, J. W.; Cardoso, S. P.; Barbosa, A. G. H.; Laali, K. K.; Rasul, G.; Prakash, G. K. S.; Olah, G. A. Unified mechanistic concept of electrophilic aromatic nitration: convergence of computational results and experimental data. *J. Am. Chem. Soc.* **2003**, *125*, 4836–4849.

[28]. Nieves-Quinones, Y.; Singleton, D. A. Dynamics and the regiochemistry of nitration of toluene. *J. Am. Chem. Soc.* **2016**, *138*, 15167–15176.

[29]. Peluso, A.; Del Re, G. On the occurrence of an electron-transfer step in aromatic nitration. *J. Phys. Chem.* **1996**, *100*, 5303–5309.

[30]. Chen, L.; Xiao, H.; Xiao, J.; Gong, X. DFT study on nitration mechanism of benzene with nitronium ion. *J. Phys. Chem. A* **2003**, *107*, 11440–11444.

[31]. Parker, V. D.; Kar, T.; Bethell, D. The polar mechanism for the nitration of benzene with nitronium ion: ab initio structures of intermediates and transition states. *J. Org. Chem.* **2013**, *78*, 9522–9525.

[32]. Koleva, G.; Galabov, B.; Hadjieva, B.; Schaefer, H. F., 3rd; Schleyer, P. von R. An experimentally established key intermediate in benzene nitration with mixed acid. *Angew. Chem. Int. Ed Engl.* **2015**, *54*, 14123–14127.

[33]. Liljenberg, M.; Stenlid, J. H.; Brinck, T. Mechanism and regioselectivity of electrophilic aromatic nitration in solution: the validity of the transition state approach. *J. Mol. Model.* **2017**, *24*, 15.

[34]. Frisch, M. J.; Trucks, G. W.; Schlegel, H. B.; Scuseria, G. E.; Robb, M. A.; Cheeseman, J. R.; Montgomery, J. A.; Vreven, T.; Kudin, K. N.; Burant, J. C.; Millam, J. M.; Iyengar, S. S.; Tomasi, J.; Barone, V.; Mennucci, B.; Cossi, M.; Scalmani, G.; Rega, N.; Petersson, G. A.; Nakatsuji, H.; Hada, M.; Ehara, M.; Toyota, K.; Fukuda, R.; Hasegawa, J.; Ishida, M.; Nakajima, T.; Honda, Y.; Kitao, O.; Nakai, H.; Klene, M.; Li, X.; Knox, J. E.; Hratchian, H. P.; Cross, J. B.; Adamo, C.; Jaramillo, J.; Gomperts, R.; Stratmann, R. E.; Yazyev, O.; Austin, A. J.; Cammi, R.; Pomelli, C.; Ochterski, J. W.; Ayala, P. Y.; Morokuma, K.; Voth, G. A.; Salvador, P.; Dannenberg, J. J.; Zakrzewski, V. G.; Dapprich, S.; Daniels, A. D.; Strain, M. C.; Farkas, O.; Malick, D. K.; Rabuck, A. D.; Raghavachari, K; Foresman, J. B.; Ortiz, J. V.; Cui, Q.; Baboul, A. G.; Clifford, S.; Cioslowski, J.; Stefanov, B. B.; Liu, G.; Liashenko, A.; Piskorz, P.; Komaromi, I.; Martin, R. L.; Fox, D. J.; Keith, T.; Al-Laham, M. A.; Peng, C. Y.; Nanayakkara, A.; Challacombe, M.; Gill, P. M. W.; Johnson, B.; Chen, W.; Wong, M. W.; Gonzalez, C.; Pople, J. A. Gaussian 16, revision B0.1., Gaussian, Inc., Wallingford CT, 2004.

[35]. Henderson, T. M.; Izmaylov, A. F.; Scalmani, G.; Scuseria, G. E. Can short-range hybrids describe long-range-dependent properties? *J. Chem. Phys.* **2009**, *131*, 044108.

[36]. Galano, A.; Alvarez-Idaboy, J. R. Kinetics of radical-molecule reactions in aqueous solution: a benchmark study of the performance of density functional methods. *J. Comput. Chem.* **2014**, *35*, 2019–2026.

[37]. Zhao, Y.; Truhlar, D. G. The M06 suite of density functionals for main group thermochemistry, thermochemical kinetics, noncovalent interactions, excited states, and transition elements: two new functionals and systematic testing of four M06-class functionals and 12 other functionals. *Theor. Chem. Acc.* **2008**, *120*, 215–241.

[38]. Shi, H. A solvent-catalyzed four-molecular two-path solvolysis mechanism of t-butyl chloride or bromide in water or alcohol derived by density functional theory calculation and confirmed by high-resolution electrospray ionization-mass spectrometry. *React. Kinet. Mech. Catal.* **2020**, *129*, 583–612.

[39]. Fukui, K.; Yonezawa, T.; Shingu, H. A molecular orbital theory of reactivity in aromatic hydrocarbons. *J. Chem. Phys.* **1952**, *20*, 722–725.

[40]. Fukui, K.; Yonezawa, T.; Nagata, C.; Shingu, H. Molecular orbital theory of orientation in aromatic, heteroaromatic, and other conjugated molecules. *J. Chem. Phys.* **1954**, *22*, 1433–1442.

[41]. Fukui, K. *Frontier orbitals and reaction paths: Selected papers of Kenichi Fukui: Selected papers of Kenichi Fukui*; Fukui, K., Ed.; World Scientific Publishing: Singapore, Singapore, 1997.

[42]. Coulson, C. A. *Coulson 's Valence*; 3rd ed.; Oxford University Press: London, England, 1979.

[43]. Barone, V.; Cossi, M.; Tomasi, J. Geometry optimization of molecular structures in solution by the polarizable continuum model. *J. Comput. Chem.* **1998**, *19*, 404–417.

[44]. Barone, V.; Cossi, M. Quantum calculation of molecular energies and energy gradients in solution by a conductor solvent model. *J. Phys. Chem. A* **1998**, *102*, 1995–2001.

[45]. Cancès, E.; Mennucci, B.; Tomasi, J. Analytical derivatives for geometry optimization in solvation continuum models. II. Numerical applications. *J. Chem. Phys.* **1998**, *109*, 260–266.

[46]. Tomasi, J.; Mennucci, B.; Cammi, R. Quantum mechanical continuum solvation models. *Chem. Rev.* **2005**, *105*, 2999–3093.

[47]. Belson, D. J.; Strachan, A. N. Aromatic nitration in aqueous nitric acid. *J Chem Soc Perkin Trans 2* **1989**, 15–19.

[48]. Zhao, Y.; Schultz, N. E.; Truhlar, D. G. Design of density functionals by combining the method of constraint satisfaction with parametrization for thermochemistry, thermochemical kinetics, and noncovalent interactions. *J. Chem. Theory Comput.* **2006**, *2*, 364–382.

[49]. Zhou, X.; He, C.; Zhang, Z.; Cao, C. Experimental investigation on nitration of benzene at different molar ratio of sulfuric acid and nitric acid, *J. Qinghai Univ.* **2010**, *2010* (4), 12-15.

[50]. Winkler, F. J. Reaction rates of isotopic molecules. VonL. Melander und W. H. saunders, Jr. Wiley, New York 1980. XIV, 391 S., geb. £ 16.30. *Angew. Chem. Weinheim Bergstr. Ger.* **1981**, *93*, 220–220.